Penerbit Akademia Baru

CFD Letters

Journal homepage: www.akademiabaru.com/cfdl.html
ISSN: 2180-1363

Numerical Investigation Of Possibility Of Using Shape Memory Alloy In Louvered Fins Radiators

Open Access

Khobib Abdelhafeiz Mohamed [1], Obai Younis [2,*], Ahmed Kadhim Hussein[3]

[1] Department of Mechanical Engineering, Faculty of Engineering, University of Khartoum, Sudan.
[2] Department of Mechanical Engineering, College of Engineering at Wadi Addwaser, Prince Sattam Bin Abdulaziz University, KSA.
[3] College of Engineering, Mechanical Engineering Department, University of Babylon, Babylon city, Iraq.

ARTICLE INFO

Article history:
Received 5 February 2019
Received in revised form 6 March 2019
Accepted 12 March 2019
Available online 23 March 2019

ABSTRACT

The objective of the present work is to enhance the heat transfer rate in an automotive radiator by using the shape memory alloy as an active louvered fin. This study presents fruitful details of the numerical study which were obtained by solving the two-dimensional Navier-Stokes equations by using ANSYS Fluent 14.0. A two-dimensional model was constructed and a standard k-epsilon model was used for the turbulence modelling. Nine heat exchangers differing in values of the fin pitch, louver angle and louver walls temperature were simulated by using a commercial CFD code ANSYS FLUENT 14 to find the best angles of the louvered fins. The obtained results were validated against experimental data which was in a reasonable agreement taking into account the computational limitations. The results indicated that the optimum angle for louver fins is independent of louver walls temperature, while it depends on the fin pitch and Reynolds number. For fin pitch of 1.65 mm, the optimum angle is 40^{o} and for fin pitch of 2.02 mm and 3.25 mm the optimum angle is 27^{o}. Therefore, the application of the shape memory alloy is not required to enhance the heat transfer rate in an automotive radiator.

Keywords:
Heat transfer, Numerical analysis, Shape memory alloy, Louvered fins, Automotive radiator.

1. Introduction

Louver fins (Figure 1 and 2) are used widely for industrial heat exchangers, air-conditioning as well as automotive radiator, heater, oil coolers, and condenser. The underlying behaviour of the air flow through louvered fin array as well as its associated pressure distribution reflects the amount of the heat transfer and the overall pressure drop. These parameters can be obtained from the experiment in relation to the geometric parameters of louvered fin.

In the past, experimental tests were performed by using wind tunnels requiring expensive instrument and tools with great difficulties on accuracy because of the complexity in the flow shape during the past two decades. A lot of researchers have studied this problem extensively. Davenport

* *Corresponding author.*
E-mail address: oubeytaha@hotmail.com (Obai Younis)

[1] performed an overall heat transfer experiments on about 32 non-standard geometries of louvered fin heat exchangers. Achachia and Cowell [2] presented an experimental data of the overall heat transfer and the friction factor for 15 variants of louvered fin geometries. Beauvais [3] performed an experiment on scaled-up louvered fin geometries. All these authors showed that the flow quickly turned to louver directed as it was entered louver geometry [1-3]. Davenport [4] repeated the flow field observations of Beauvais [3] and it was concluded that, the degree of the louver directed flow was a function of Reynolds number. The flow field measurements carried by Springer [5] and Springer and Thole [6 - 7] showed in detail the manner in which the fluid entered and changed to the axial direction as it passed through the louver array. It was found that the length required achieving the fully developed flow increased with increasing the fin pitch. Zhang *et al.,* [8] solved computational models of the heat transfer enhancement mechanisms of in-line and staggered parallel plates in heat exchangers that simulated the infinite arrays in all directions. Kurosaki *et al.,* [9] carried out an experimental study on the heat transfer from parallel louvered fins by using the Laser Holographic Interferometry. The effects of thermal wakes on the heat transfer of downstream louvers in various arrangements of parallel plates were investigated. Sparrow and Hajiloo [10] studied experimentally the heat transfer performance and the pressure drop for an array of staggered plates aligned parallel to an air flow. During different experiment the plate thickness and Reynolds number varied parametrically. It was concluded that the heat transfer coefficient and friction factor increase with plate thickness for all ranges of Reynolds numbers. Webb *et al.,* [11], presented an experimental data for six brazed aluminium heat exchangers. The heat transfer and the friction factor correlation for the louver fin geometry are suggested. The heat transfer data for the Colburn j-factor are correlated within 10%, and those for the friction factor are within 15%. Sunden and Svantesson [12], investigated the thermal and hydraulic performance of a multi-louvered fins. It was found that, every configuration of louvered surfaces which are studied were more efficient than the corresponding plain surface. Chang and Wang [13] presented 27 samples of corrugated louvered fin heat exchangers with different geometrical parameters. A generalized heat transfer correlation for Louver fin geometry was deduced. Andrew [14] spatially re-solved the heat transfer studies in Louvered fins for compact heat exchangers. He presented an experimental data and solved the computational model for six scaled up louvered fin geometries. He found that for, louver angle $\theta = 27^{o}$ and ratio of fin pitch to louver pitch $F_p/L_p = 1.52$ geometry performed the best performance at $Re_{Lp} = 230$ mm and $Re_{Lp} = 370$ mm respectively. While, for $\theta = 39^{o}$ and $F_p/L_p = 0.91$ geometry gave the best performance at $Re_{Lp} = 1016$. Jiin and Ying [15] presented an experimental data and a numerical investigation for 3D computational fluid dynamics model. They searched for optimum louver angles design for a louvered fin heat exchanger. They concluded that the angle ranging from $\theta = 15^{o}$ to 45^{o} was acceptable for suitable louver pitches and Reynolds number.

Computational Fluid Dynamic (CFD) has been widely used recently and considered a successful tool for understanding the flow and heat phenomena in many heat transfer devices. Numerical studies aimed to enhance the heat transfer rate were recommended in automotive radiator by using the shape memory alloy as an active louvered fin. Shape memory alloys are a unique class of metal alloys that can recover the apparent permanent strains when they are heated above a certain temperature. They have two stable phases - the high–temperature phase, called austenite and the low–temperature phase, called martensite [16].Alloys are available in ternary Cu-Zn-Al and Cu-Al-Ni alloys, or in their quaternary modifications containing manganese. Shape memory alloys can be processed to remember both hot and cold shapes. They can be cycled between two different

shapes without the need of external stress [17]. Elements such as boron, cerium, cobalt, iron, titanium, vanadium, and zirconium are also added for grain refinement [18]. B. Ameel *et al.,* [19] numerically investigated the effect of individually varying louver angles and fin geometry on heat transfer performance of a round. They concluded that an increment of 1.3% in the Colburn j factor is obtained for the same value of friction factor when utilizing varying louver angles. Experimental and parametric analysis on thermo-hydraulic performance of louvered fin and flat tube heat exchanger is carried out by V. Karthik *et al.,* [20]. Their results indicated that the pressure drop increases with the decrease in fin pitch, the increase in both transverse and longitudinal tube pitches and the reduction of the louver pitch. On the other hand the connective heat transfer is not affected by the transverse and longitudinal tube pitches while it is increased fin pitch. Jie Deng [21] used the large eddy simulations (LES) to investigate flow and heat transfer characteristics of the large size multi-louvered fin arrays with various structural parameters. He succeeded in presenting new modified correlations with higher accuracy than the correlations reported in the literature. Numerical modelling and simulations of car radiator is conducted by Kabir B. S. et. al. [22], in this research the effect of fins under the atmospheric condition of Kano, Nigeria is presented. The authors concluded that the atmospheric condition has a great influence on car radiator performance; precisely under Kano weather conditions the fins increase the cooling efficiencies of the radiators up to 77%.

The present paper has two major focuses relative to the performance of the louvered fin compact heat exchanger .The first is to determine the effect of louver walls temperature on the optimum louver angle (the angle obtained by balancing efficient heat transfer with reasonable pressure drops). The second purpose is to study the ability of using shape memory alloys as an active louvered fin to improve the heat transfer rate. To reach this goal, nine heat exchangers differing in values of fin pitch, louver angle and louver walls temperature were simulated by a using commercial CFD code ANSYS FLUENT 14 to find the best angles of the louvered fins. Figure 1 illustrates the typical louvered fin and the tube heat transfer unit, while Figure 2 shows the side view of typical louvered fin geometry including the louver inlet flow direction and louvered fin terminology. As shown in Figure 2 the gap between two louvered fins is called fin pitch (F_p), the length from the leading edge to the end of the fin is call flow depth (F_d), the horizontal length of the gap between two successive louvers is called louver pitch (L_p), all the previous lengths are measured in mm. In Figure 3 the one-way and two-way shape memory effects are illustrated.

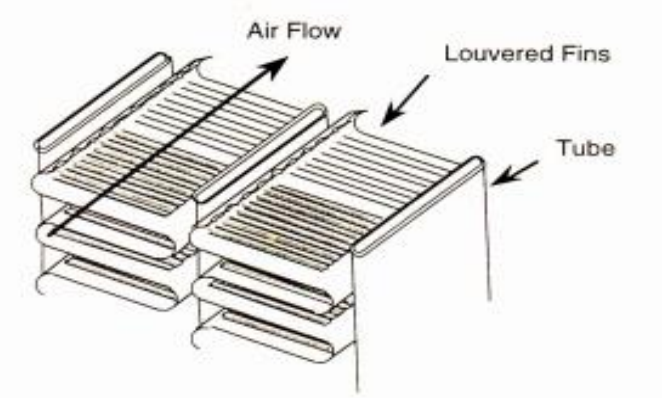

Fig. 1. Typical louvered fin and the tube heat transfer unit

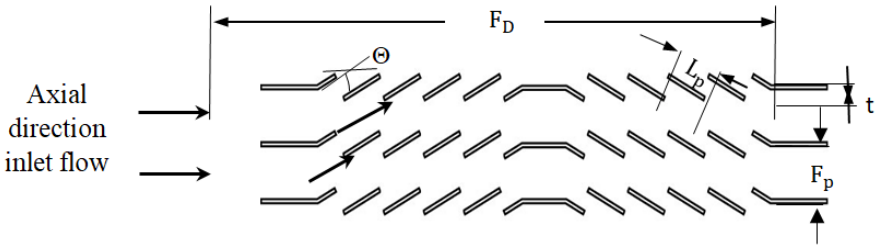

Fig. 2. Side view of typical louvered fin geometry

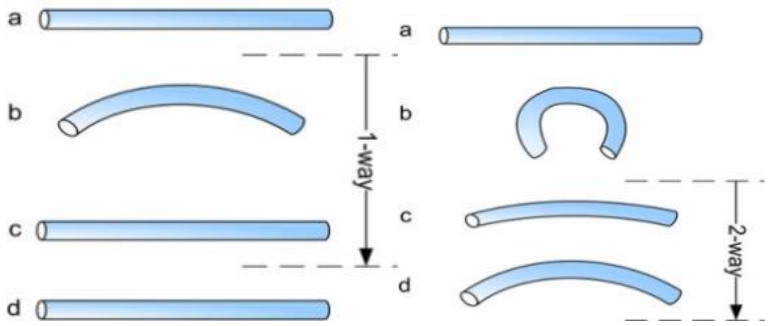

Fig. 3. One-way and two-way shape memory effect (a) Starting from Martensite (b) Adding a reversible deformation for the one-way effect or severe deformation with an irreversible amount for the two-way (c) Heating (d) Cooling

2. Methodology

2.1. Geometrical Parameter of Louver Fins

The geometrical parameters for plate-fin geometry in the present study are shown in Figure 4. All samples in this analysis have the louver pitch of (1.4 mm) and fin thickness of (0.05 mm). Simulations are performed for different geometries with various fin pitch (F_p), louver angle (θ) and louver temperature (T_{louver}). The values of these parameters are listed in Table 1. The scope of this paper is based on configurations and louver parameters reported by Pega *et al.,* [23], including three different values of louver angle and fin pitch.

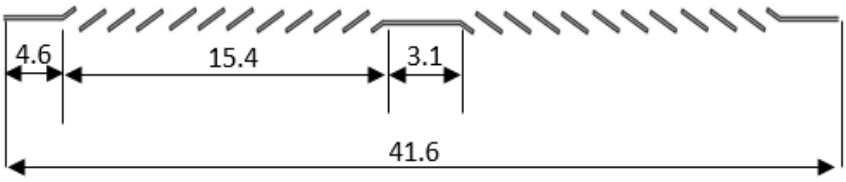

Fig. 4. Geometrical parameters of the louvered plate-fin geometry (mm)

Table 1
Geometric parameters and test cases for the louver fin models

Test section number	1	2	3	4	5	6	7	8	9
Fin pitch (F_P) (mm)	1.65			2.02			3.25		
Louver angle (θ)	15°	27°	39°	15°	27°	39°	15°	27°	39°

Louver temperature (T_{louver}) (°C)	85 95 105	85 95 105	85 95 105
Louver Pitch (L_p) (mm)	1.4	1.4	1.4
Louver Thickness ,t (mm)	0.05	0.05	0.05
Inlet Velocity V_{in} (m/s)	3	3	3

2.2. Boundary Conditions and Computational Details

The numerical simulations are performed for three different temperatures of louver surface which are 358, 368 and 378 K. The inlet air temperature of the louver fin is kept at 300 K and with a velocity of 3 m/s [14] (trouble of cooling for radiators occurs at the low speed). All the thermo-physical properties of the air and fin surface (Specific heat at constant volume C_v , Specific heat at constant pressure C_p, density ρ, kinematic viscosity ν and louver thermal conductivity k) are assumed to be constant.

The computational model was specified to be two-dimensional, turbulent, and steady with a heat transfer. Computations were performed on a model consisting of a single periodic fin row model which has 23 stream wise louvers. Periodic boundary conditions were specified on the upper and lower edges of the model. Inlet uniform velocity was specified at the entrance of the fin row and an outlet pressure condition was specified at the exit of the fin row.

The SIMPLE algorithm [24] is used to couple the fluid pressure and velocity. The discretization of momentum, turbulence, kinetic energy, turbulence dissipation rate, and energy equations are set by QUICK scheme [24]. Different values for under relaxation factors are set as the followings: for pressure correction equation = 0.3, momentum equation = 0.7, turbulence kinetic energy equation = 0.8, turbulence dissipation = 0.8 and energy = 1. The residual for converged solution of the continuity, component of velocity, turbulence kinetic energy and turbulence dissipation rate are below (10^{-3}) , while for energy is below (10^{-6}).

A quadrilateral mesh was used over the entire model with refine mesh around the boundaries of the louvers. A detail of a portion of this grid highlighting the quadrilateral mesh around the louvers is shown in Figure 5. While, Figure 6 shows the prediction of the heat transfer solution for several meshes at θ = 15°.The final model contained 31,455 cells with skewness value of 0.39 and Y^+ ranges between 175 and 350.

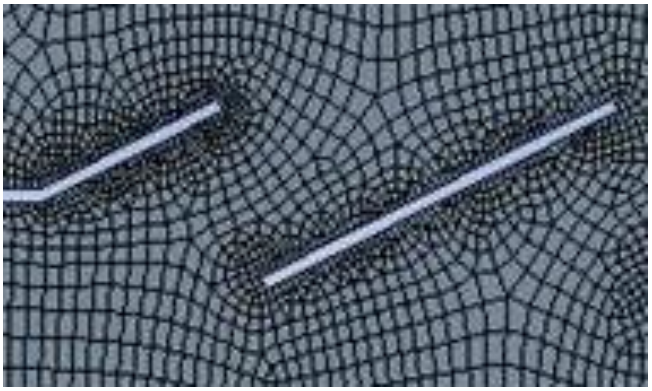

Fig. 5. Portion of CFD mesh used for case with a single row and periodic flow boundary condition

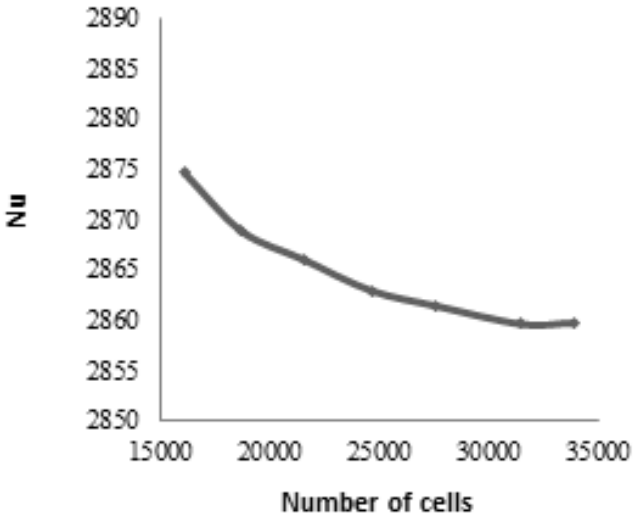

Fig. 6. The variation of Nusselt number with various mesh sizes for F_P =2.02 mm, θ= 15° and T_{louver} =358 K

2.3. Governing Equations

Due to the low relative velocity, the fluid is considered incompressible with constant properties and the flow is assumed to be turbulent, steady, and two-dimensional. The dimensionless governing equations for mass, momentum (Navier-Stokes equation) and energy may be expressed in tensor form as follows:

Continuity Equation [24]

$$\nabla.\left(\rho\vec{V}\right) = 0 \tag{1}$$

Where ρ is the density and V is the velsocity.

Conservation of momentum (Navier-Stokes Equations)
Cauchy's equation [24]

$$\nabla.\left(\rho\vec{V}\vec{V}\right)=\rho\vec{g}+\vec{\nabla}.\sigma_{ij} \tag{2}$$

Where (σ_{ij}) is the stress tensor, which can be separated into the pressure stresses and the viscous stresses as follows [24]

$$\sigma_{ij}=\begin{pmatrix}\sigma_{xx}\sigma_{xy}\sigma_{xz}\\ \sigma_{yx}\sigma_{yy}\sigma_{yz}\\ \sigma_{zx}\sigma_{zy}\sigma_{zz}\end{pmatrix}=\begin{pmatrix}-p & 0 & 0\\ 0 & -p & 0\\ 0 & 0 & -p\end{pmatrix}+\begin{pmatrix}\tau_{xx}\tau_{xy}\tau_{xz}\\ \tau_{yx}\tau_{yy}\tau_{yz}\\ \tau_{zx}\tau_{zy}\tau_{zz}\end{pmatrix} \tag{3}$$

where p is the pressure stress and τ is the viscous stress.

Incompressible Navier-Stokes equation is given by [24]

$$-\nabla p+\rho\vec{g}+\mu\nabla^2\vec{V}=0 \tag{4}$$

where g is gravity and μ is the dynamic viscosity.

Conservation of energy is given by [24]

$$\rho\frac{\partial}{\partial t}\left(C_v T+\frac{V^2}{2}\right)+\rho\vec{V}.\nabla\left(C_v T+\frac{V^2}{2}\right)$$
$$=\rho g.\vec{V}-\nabla.p\vec{V}+\nabla.\left[2\mu\nabla\left(\frac{V^2}{2}\right)+\mu(\nabla\times\vec{V})\times\vec{V}-\frac{2}{3}\mu(\nabla.\vec{V})\times\vec{V}\right]+\nabla.k\nabla T \tag{5}$$

2.4. Turbulence Modelling

The *k-ε* model is the most popular two-equation model. It is based mainly on the exact transport equation of the kinetic energy (*k*) and the dissipation rate (*ε*) .The *ε* equation was chosen to determine the turbulent length scale (*l*) model as it appears naturally in the *k* equation. The turbulent eddy viscosity is obtained by choosing ($k^{1/2}$) to be the velocity scale and (k/ε) to be the time scale. The model equations can be written as follows [23 and 24]:

$$U_j\frac{\partial k}{\partial x_j}=\left(\left(\nu+\frac{\nu_t}{\sigma_k}\right)\frac{\partial k}{\partial x_j}\right)+P_k-\varepsilon \tag{6}$$

$$U_j\frac{\partial \varepsilon}{\partial x_j}=\left(\left(\nu+\frac{\nu_t}{\sigma_\varepsilon}\right)\frac{\partial \varepsilon}{\partial x_j}\right)+\frac{C_{\varepsilon_1}P_k}{T}-\frac{C_{\varepsilon_2}\varepsilon}{T} \tag{7}$$

The velocity is given by :- $\nu=k^{\frac{1}{2}}$

the eddy viscosity is given by: - $\nu_t=C_u\frac{k^2}{\varepsilon}$

The length scale is given by:- $l=\frac{k^{3/2}}{\varepsilon}$

The closure coefficients are given by :- $C_{\varepsilon_1}=1.44,\ C_{\varepsilon_2}=1.92,\ C_\mu=0.09,\ \sigma_k=1,\ \sigma_\varepsilon=1.3$

The local heat transfer coefficient (h) is defined as:

$$h = \frac{q''}{T_{louver} - T_b} \tag{8}$$

Where (q'') is the local heat flux and (T_b) is the local bulk mean temperature of the fluid. The local heat transfer coefficient can be expressed in the dimensionless form in terms of the Nusselt number (Nu), which is defined as:

$$Nu = \frac{h \cdot F_p}{k} = \frac{\partial \left[\frac{\Theta}{\Theta_b}\right]_{wall}}{\partial n} \tag{9}$$

Where (F_p) is the fin pitch and (k) is the thermal conductivity respectively. Also, $\Theta = (T-T_{in}) / (T_w-T_{in})$ is the dimensionless temperature, $\Theta_b = (T_b-T_{in}) / (T_w-T_{in})$ is the local dimensionless bulk mean temperature, and (n) is the dimensionless unit vector normal to the wall.

The average Nusselt number ($\overline{Nu}$) can be obtained by:

$$\overline{Nu} = \frac{\int Nu \quad dh}{\int dA} \tag{10}$$

where (dA) is the infinitesimal area of the wall surface.

3. Validations

To ensure the validity and accuracy of the calculations, the louvered fin simulation results are compared with the available experimental data of Andrew [14]. The specifications of the models and test conditions are shown in Table 2. Moreover, Figure 7 shows two heat transfer curves which present the variation of the heat transfer coefficient represented by the Nusselt number with the length of front side of second louver in array. The first curve was measured experimentally and the other one was predicted by CFD simulation. In order to experimentally measure a heat transfer profile is close to the one predicted by the CFD model. The difference is expected as a normal computer (Laptop, Intel CORE i5) was used and number of simplifying assumptions that limit the accuracy of CFD results.

Table 2
Geometric parameters and test cases for the louver fin models

Test Section Number	1
θ	27°
Louver pitch (L_p), (m)	0.0279
Ratio of fin pitch to louver pitch (F_p/L_p)	0.76
Ratio of fin thickness to louver pitch (t/L_p)	0.082
Nozzle number used	1
Reynolds numbers tested (Re_{Lp})	230
Test section inlet area (m^2)	0.0381
Minimum free flow area, (A_{ff})(m^2)	0.0341

Heat flux boundary condition (W/ m^2)	60
Maximum mass velocity, G (kg/s m)	0.151
Inlet velocity (m/s)	0.13

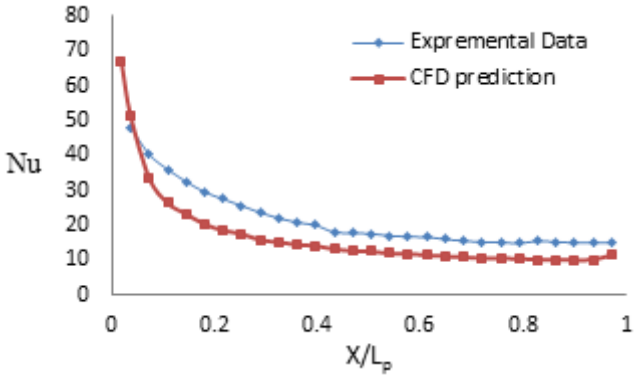

Fig. 7. Comparison of experimental data and the numerical predictions of the Nusselt number in the front side of louver 2

4. Results

4.1. Flow Aerodynamic and Temperature Distribution

Figure 8 and 9 show the results of velocity and temperature contours for three different louver angles with fin pitch F_P = 2.02 mm, louver surface temperature T_{louver} = 358 K and inlet velocity V_{in} = 3 m/s. It can be seen from results presented in Figure 8 (a) and (b) that, for small louver angle some of the flow stream passes the louver passages and flows as "duct flow", between the fin channels. Therefore, the heat exchanger performance is then close to that of a plain duct, and the louvers are relatively ineffective. Now , when the louver angle increases [Figure 8 (c)] , the fin spacing decreases and the hydraulic resistance in the louver direction decreases with respect to the axial direction due to the increase in the friction factor and the pressure drop along the duct flow path. This leads to more flow will pass through the louver direction and implies a higher "flow efficiency" [23]. Generally, the temperature difference between the fin surface and the air is much at the entrance of the louver fin. Therefore, the heat transfer rate is high as shown in Figure 9. Gradually the temperature difference is reduced along the louver array. Also, it can be seen that the results of the heat transfer performance of the fin is poor at the exit.

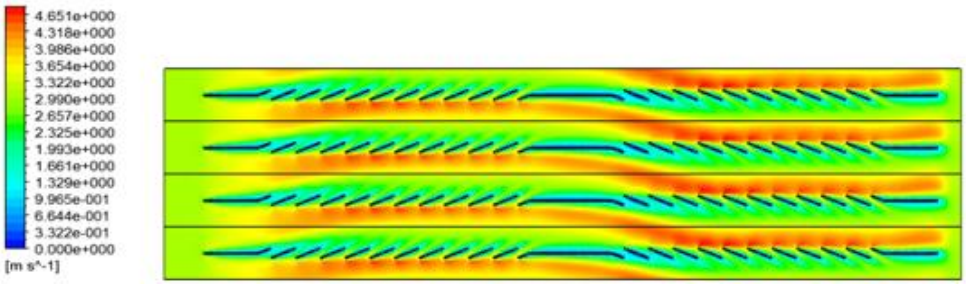

(a) Velocity contours (m/s), θ = 15°

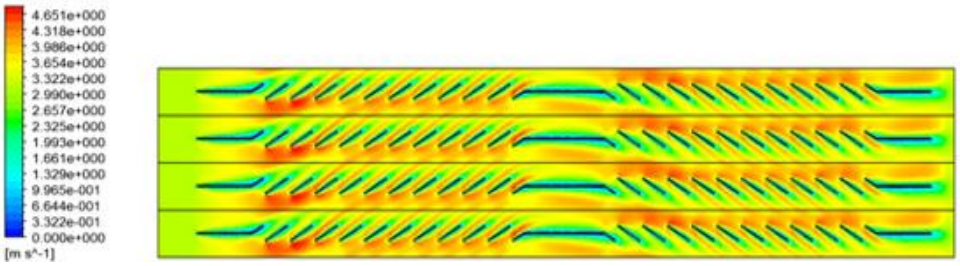

(b) Velocity contours (m/s), θ = 27°

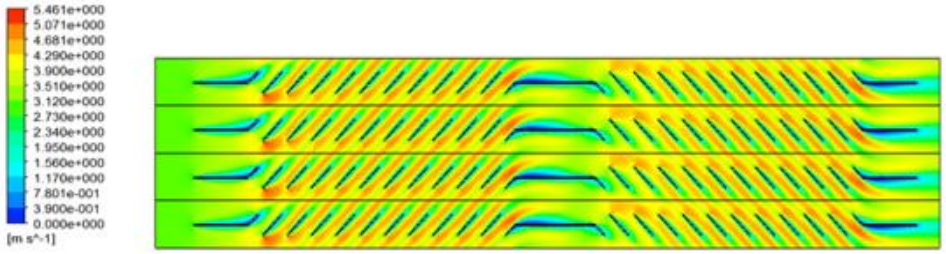

(c) Velocity contours (m/s), θ = 39°

Fig. 8. Velocity contours for three louver angles at [F_P = 2.02 mm and T_{louver} = 358 K]

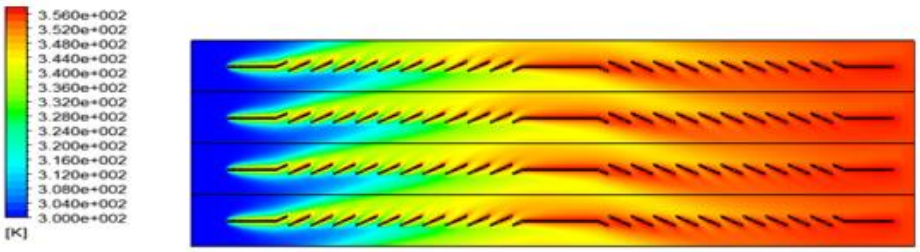

(a) Temperature contours (K), θ = 15°

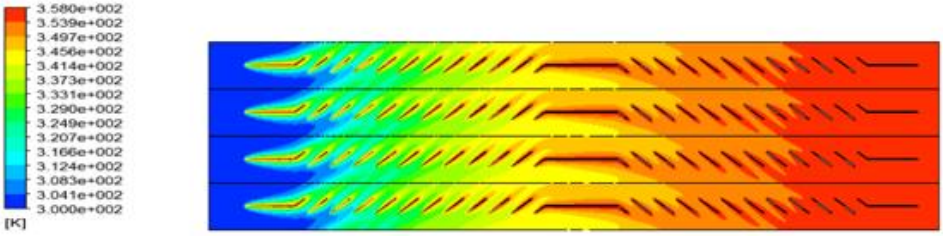

(b) Temperature contours (K), θ = 27°

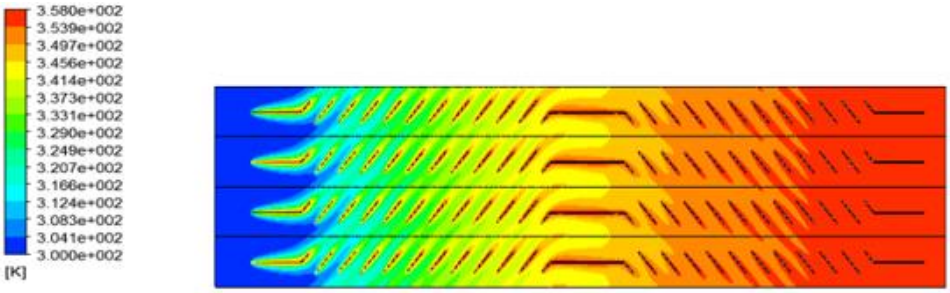

(c) Temperature contours (K), θ = 39°

Fig. 9. Temperature contours for three louver angles at [F_P = 2.02 mm and T_{louver} = 358 K]

4.2. Effect of the Louver Angle on the Heat Transfer Coefficient

Nine models of F_P = 1.65, 2.02 and 3.25 mm and θ = 15° , 27° and 39° were simulated with a constant louver temperature [T_{louver} = 358 K] . The variation of the heat transfer with the louver angle was plotted in Figure 10 to specify the optimum angle for any fin pitch. This figure shows that, the heat transfer coefficient increases with the small louver angle (less than 27° in this case), but for the greater one, the overall heat transfer coefficient varies with the fin pitch [i.e., F_P = 1.65, 2.02 and 3.25 mm].

For (F_P =1.65 mm), the heat transfer coefficient increases slightly with the louver angle and for (FP = 3.25 mm) it almost has the same value, but for (FP = 2.02 mm), it decreases with the louver angle greater than 27°.

This indicates that for a given geometry and operating conditions, the maximum heat transfer performance occurs at louver angle of θ = 27°. The overall heat transfer coefficient for the case with a louver angle θ = 27° and fin pitch equals to 2.02 mm is 1.12 % higher than the case with a louver angle θ = 15°, and is 16.32 % higher than the case with a louver angle θ = 39°. This is mainly due to the lower flow efficiency (high pressure drop) for the case with θ = 39°.

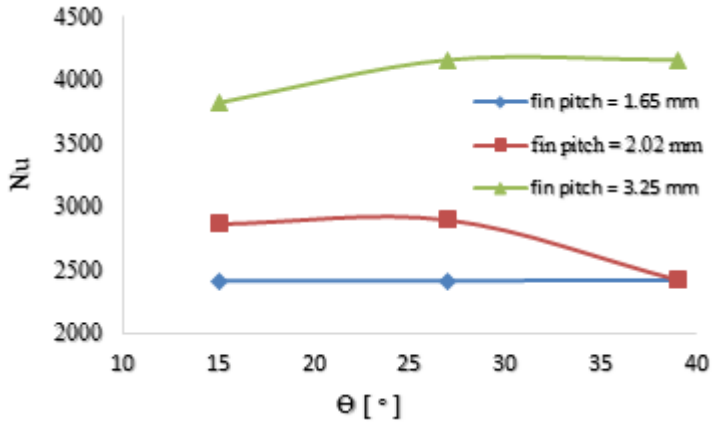

Fig. 10. Variations of the Nusselt number with louver angle for three different fin pitches and T_{louver}=358 K

4.3. Effect of the Louver Angle on the Air Side Pressure Drop

Figure 11 presents the pressure drop data for the multi-louvered fin heat exchangers with different louver angles, 15° , 27° and 39°, the fin pitches 1.65, 2.02, and 3.02 mm and louver walls temperature equals to T_{louver}= 358 K. It can be seen that, the pressure drop increases with the louver angle for all fin pitches and also the gradient increased. The increment of the pressure drop causes higher mass flow rate of the air through the system which results in higher rates of heat transfer and hence higher values of Nusselt number (Figure 10). For the fin equals to *FP* = 2.02 mm , the pressure drop for the louver angle θ = 27° is about 18.16 % higher than θ = 15° and its about 77.5 % lower than θ = 39°.

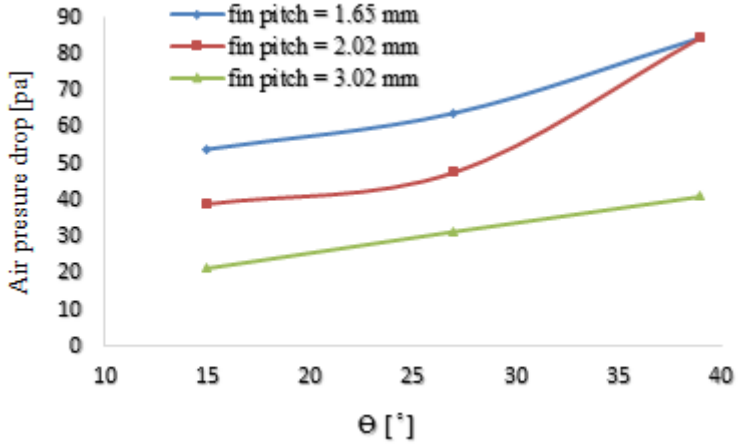

Fig. 11. Variations of air-side pressure drops with the louver angle for three different fin pitches and T_{louver}=358 K

4.4. Effect of the Louver Walls Temperature on the Optimum Angle

The Shape Memory Alloy (SMA) has characteristic which can be trained to modify its position with variation of the temperature. So, the variation of the heat transfer coefficient against the louver angle was plotted for louver temperatures T_{louver} = 358, 368 and 378 K, and fin pitches F_p =1.65 and 2.02 mm as shown in Figure 12 and 13 respectively. The purpose of these figures is to examine the dependency of the optimum angle on the louver temperature.

The results indicated that, the variation of louver walls temperatures does not affect the trend of the heat transfer coefficient curves except that they rise up. It is well known that the heat transfer rate is proportional to temperature difference; however the results showed that the general trend of the heat transfer coefficient is not affected by the value of louver wall temperature while it is strongly affected by the louver angle and/or fin pitch. For small relative values of fin pitch (F_p=1.65 mm), the effect of louver angle variation on the heat transfer coefficient is minimal (Figure 13). In such cases, the relatively small fin spacing causes the fluid to flow as duct flow [23] and hence the louvered will be less effective and the louver angle effects are supressed. On the other hand, the effects of louver angle variation clearly presents for higher values of fin pitch (F_p2.02 and 3.25 mm) (Figure 12). The optimum louver angle for F_p=1.65 equals to θ = 40^o and for F_p= 2.02 equals to θ = 27^o.

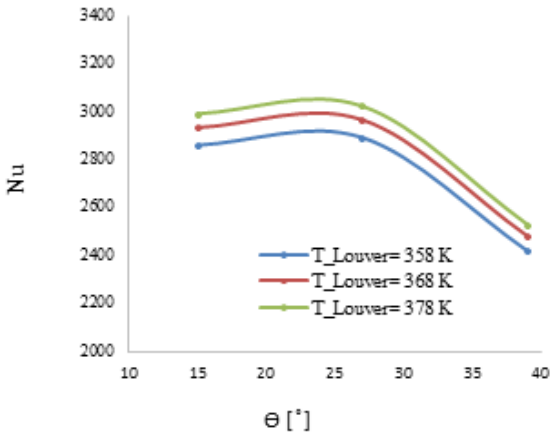

Fig. 12. Variations of Nusselt number with louver angle for three different louver temperature at F_p= 2.02 mm

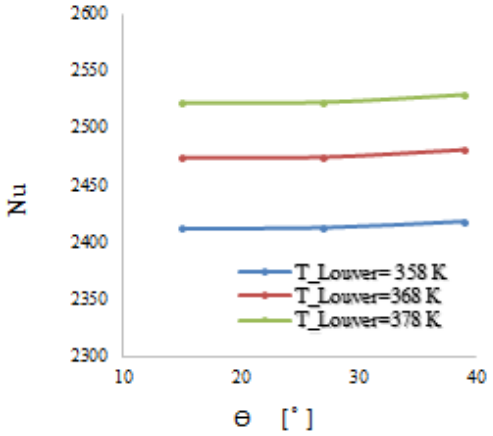

Fig. 13. Variations of Nusselt number with louver angle for three different louver temperature at F_p= 1.65 mm

5. Conclusion

Optimum louver angle was studied by considering the heat transfer and friction loss of louver plate fins in terms of the Nusselt number and the pressure drop. The study is performed within a range of the three fin pitches (F_p = 1.65, 2.02 and 3.25 mm) and louver angle θ = 15°, θ = 27° and 39° which are similar to Pega *et al.,* [23]. Numerical simulations were performed for all nine models. If there is a different optimum angle for each value louver wall temperature, then the shape memory alloy can be trained and used as active louvered fin to change its position to match the optimum angle depending on the louver wall temperature. From the results, it can be concluded that:

a) For F_p= 1.65 mm, the optimum angle equals to θ = 40° and for F_p= 2.02 and 3.25 mm it's equals to θ = 27°.
b) Optimum louver angle is independent of the louver walls temperature, but it depends on the fin pitch.
c) The application of Memory shape alloy in in louvered fin radiators is not applicable since the optimum louver angle is independent of louver wall temperature.

References

[1] Davenport, C. J. "Correlation for heat transfer and flow friction characteristics of louvered fin." In *AIChE Symp. Ser*, vol. 79, no. 25, pp. 19-27. 1983.
[2] Achaichia, A., and T. A. Cowell. "Heat transfer and pressure drop characteristics of flat tube and louvered plate fin surfaces." *Experimental Thermal and Fluid Science* 1, no. 2 (1988): 147-157.
[3] Beauvais, F. N. *An aerodynamic look at automotive radiators*. No. 650470. SAE Technical Paper, 1965..
[4] Davenport, Christopher John. "Heat transfer and fluid flow in louvred triangular ducts." PhD diss., Coventry Polytechnic, 1980.
[5] Springer, Marlow E., and Karen A. Thole. "Experimental design for flowfield studies of louvered fins." *Experimental Thermal and Fluid Science* 18, no. 3 (1998): 258-269.
[6] Springer, Marlow E., and Karen A. Thole. "Experimental design for flowfield studies of louvered fins." *Experimental Thermal and Fluid Science* 18, no. 3 (1998): 258-269.
[7] Springer, Marlow E., and Karen A. Thole. "Entry region of louvered fin heat exchangers." *Experimental Thermal and Fluid Science* 19, no. 4 (1999): 223-232.

[8] Zhang, L. W., S. Balachandar, D. K. Tafti, and F. M. Najjar. "Heat transfer enhancement mechanisms in inline and staggered parallel-plate fin heat exchangers." *International Journal of Heat and Mass Transfer* 40, no. 10 (1997): 2307-2325.
[9] Kurosaki, Yasuo, Takao Kashiwagi, Hiroki Kobayashi, Hideo Uzuhashi, and Shie-Chung Tang. "Experimental study on heat transfer from parallel louvered fins by laser holographic interferometry." *Experimental Thermal and Fluid Science* 1, no. 1 (1988): 59-67.
[10] Sparrow, E. M., and A. Hajiloo. "Measurements of heat transfer and pressure drop for an array of staggered plates aligned parallel to an air flow." *Journal of Heat Transfer* 102, no. 3 (1980): 426-432.
[11] Webb, R. L., Y-J. Chang, and C-C. Wang. "Heat transfer and friction correlations for the louver fin geometry." In 1995 *Vehicle Thermal Management Systems Conference Proceedings*, pp. 533-541. 1995.
[12] Sunden, Bengt, and Jerker Svantesson. "Thermal hydraulic performance of new multilouvered fins." In *Proceedings of the 9th Int. Heat Transfer Conf*, vol. 14, pp. 91-96. 1990.
[13] Chang, Yu-Juei, and Chi-Chuan Wang. "A generalized heat transfer correlation for louver fin geometry." *International Journal of heat and mass transfer* 40, no. 3 (1997): 533-544.
[14] Lyman, Andrew C. "Spatially resolved heat transfer studies in louvered fins for compact heat exchangers." PhD diss., Virginia Tech, 1999.
[15] Jang, Jiin-Yuh, and Ying-Chi Tsai. "Optimum louver angle design for a louvered fin heat exchanger." *International Journal of Physical Sciences* 6, no. 28 (2011): 6422-6438.
[16] Hodgson, Darel E., W. H. Ming, and Robert J. Biermann. "Shape memory alloys." *ASM International, Metals Handbook, Tenth Edition.* 2 (1990): 897-902.
[17] Becker, Marcus Patrick. "Thermomechanical training and characterization of shape memory alloy axial actuators." PhD diss., Montana State University-Bozeman, College of Engineering, 2010.
[18] Winit, J., Niwat, P., Seiji, O.; and Jarruwat, C. (2009). Simulation of Flow Aerodynamics and Heat Transfer in a Plate-Fin Radiator. ANSCSE 13, International College, King Mongkut's Institute of Technology Ladkrabang , March 25-27 Bangkok , Thailand.
[19] Ameel, Bernd, Joris Degroote, Henk Huisseune, Peter De Jaeger, Jan Vierendeels, and Michel De Paepe. "Numerical optimization of louvered fin heat exchanger with variable louver angles." In *Journal of Physics: Conference Series,* vol. 395, no. 1, p. 012054. IOP Publishing, 2012.
[20] Karthik, P., V. Kumaresan, and R. Velraj. "Experimental and parametric studies of a louvered fin and flat tube compact heat exchanger using computational fluid dynamics." *Alexandria Engineering Journal* 54, no. 4 (2015): 905-915.
[21] Deng, Jie. "Improved correlations of the thermal-hydraulic performance of large size multi-louvered fin arrays for condensers of high power electronic component cooling by numerical simulation." *Energy Conversion and Management* 153 (2017): 504-514.
[22] Kabir Bashir Shariff, Bala Abdullahi, and Saidu Bello Abubakar. "Modelling and Simulation of Car Radiator: Effects of Fins under the Atmospheric Condition of Kano, Nigeria." *Journal of Advanced Research in Fluid Mechanics and Thermal Sciences* 48: 1-16.
[23] Hrnjak, Pega S., Ping Zhang, and Chris Rennels. "Effect of louver angle on performance of heat exchanger with serpentine fins and flat tubes in periodic frosting." (2012).
[24] H. K. Verseeeg and W. Malalaskera. (2007). Introduction to Computational Fluid Dynamics - The Finite Volume Method. Longman Scientific & Technical, Harlow, England, Second Edition.